Date: August 1, 2014

Submitted to: Atmospheric Chemistry and Physics

Revised manuscript (minor revision)

Estimation of the direct and indirect impacts of fireworks on the physicochemical characteristics of atmospheric PM_{10} and $PM_{2.5}$

Y.Z. Tian, J. Wang, X. Peng, G.L. Shi*, Y.C. Feng

State Environmental Protection Key Laboratory of Urban Ambient Air Particulate Matter Pollution Prevention and Control, College of Environmental Science and Engineering, Nankai University, Tianjin, 300071, China

*, Correspondence author. Tel.: +862223503397; fax: +862223503397.

E-mail address: nksgl@hotmail.com (G.L. Shi).

Abstract:

To quantify the total, direct and indirect impacts of fireworks individually, size-resolved PM samples were collected before, during, and after a Chinese folk-custom festival (Chinese New Year) in a megacity in China. Through chemical analysis and morphological characterisation, a strong influence of fireworks on the physicochemical characteristics of PM_{10} and $PM_{2.5}$ was observed. The concentrations of many species exhibited an increasing trend during the heavy-firework period, especially for K^+, Mg^{2+} and Cr; and the results of the non-sea-salt ions demonstrated an anthropogenic influence on K^+ and Mg^{2+}. Then, source apportionment was conducted by receptor models and Peak Analysis. The total influence of the fireworks was quantified by PMF, showing that the fireworks contributed higher fractions (23.40% for PM_{10} and 29.66% for $PM_{2.5}$) during the heavy-firework period than during the light-firework period (4.28% for PM_{10} and 7.18% for $PM_{2.5}$). The profiles of the total fireworks obtained by two independent methods (PMF and Peak Analysis) were consistent, with higher abundances of K^+, Al, Si, Ca and OC. Finally, the individual contributions of the direct and indirect impacts of fireworks were quantified by CMB. The percentage contributions of resuspended dust, biomass combustion and direct fireworks were 36.8±8.37%, 14.1±2.82% and 44.4±8.26%, respectively, for PM_{10} and 34.9±4.19%, 16.6±3.05% and 52.5±9.69%, respectively, for $PM_{2.5}$, in terms of the total fireworks. The quantification of the total, direct and indirect impacts of fireworks in the ambient PM gives an original contribution to

understand the physicochemical characteristics and mechanisms of such high-intensity anthropogenic activities.

Keywords: PM; source apportionment; fireworks; PMF; CMB; Chinese New Year

1 Introduction

Atmospheric particulate matter (PM) is recognised globally as a major environmental issue with adverse effects on air quality, regional visibility, global climate change and health effects (Ding et al., 2008; Robichaud and Ménard, 2014). By scattering and absorbing incoming solar radiation and outgoing terrestrial radiation directly, or by acting as cloud-condensation nuclei and thereby influencing the optical properties of clouds indirectly, atmospheric aerosols can influence the radiation balance of the earth's atmosphere (Lin et al., 2013; Shen et al., 2013). Ambient PM is a complex mixture of components from a variety of sources, including natural and anthropogenic sources (Zheng et al., 2005; Zhao et al., 2013a). In recent years, concerns about short-term air quality degradation events and their continuous negative effects to human health has increased, especially for PM pollution caused by high-intensity anthropogenic activities.

Firework displays are high-intensity anthropogenic activities that create notable air pollution and obvious short-term air-quality degradation. Firework displays are used to celebrate popular fiestas, a practice common worldwide (e.g., at the New Year). During firework episodes, there is usually a transient and spectacular increase in the PM pollution. Fireworks contain a variety of metal salts, such as chlorates and perchlorates (Wang et al., 2007; Crespo et al., 2012), leading to extremely high ambient concentrations of these species during the celebration. These heavy metals and perchlorates are all highly toxic (Shi et al., 2011) and are on average fine enough to be easily inhaled and show a health risk to susceptible individuals. Both the

long-term and short-term hazardous impacts of fireworks on human health have been paid significant attention by researchers (Wang et al., 2007; Vecchi et al., 2008; Crespo et al., 2012; Cheng et al., 2013).

Studies have demonstrated that the displacement of fireworks could be an important source category for atmospheric PM (Vecchi et al., 2008). Fireworks can influence the PM directly by emitting firework-related species (such as certain heavy metals). Additionally, the accessory effects, which were indirectly caused by the activities of firework displays, should be taken into consideration in the firework events. For example, pyrotechnic device explosions can lead to resuspension of materials already deposited on the ground; and biomass combustion (fireworks are made from paper and a cracker) occurs when the fireworks are displayed and incinerated after display. Although firework-related pollution episodes are transient in nature, they are highly concentrated, and the influence is continuous. Both the direct and indirect influences of fireworks might significantly contribute to PM and the total annual metal emissions. However, the quantification of firework contributions, especially for its direct and indirect impacts, is very limited.

Studies on fireworks have mainly applied the following methods: burning fireworks in specific laboratories or fields to characterise their chemical properties (Tsai et al., 2012); and investigating the environmental impacts through ambient sampling champion during firework periods (Sarkar et al., 2010; Crespo et al., 2012). The former cannot reflect the actual ambient condition and indirect impacts. For the latter, celebrations by fireworks are usually continued for only a few days. Thus, it has been

very difficult to quantify the contributions of fireworks to ambient PM, especially for the quantification of indirect impacts. Selecting an appropriate period and site for this subject is key. Fireworks are more prevalent in certain places than others. China is the country that produces the most fireworks in the world (Shi et al., 2011). In addition, setting off fireworks is a traditional way to celebrate the Chinese New Year (CNY, Spring Festival) and is justifiably welcomed all over the country. CNY is the most important folk-custom holiday in China. Celebrations during CNY season tend to spill over into the preceding and succeeding days (usually until the Lantern Festival, another important festival in China), along with sporadic fireworks. During the firework episodes, the anthropogenic emission patterns are greatly changed (Huang et al., 2012). Many ordinary activities are decreased, such as certain industries and traffic (Feng et al., 2012), whereas degradation of the air quality might occur due to displays of fireworks. This provides a unique opportunity to study the drastic source changes and allows the quantification of the direct and indirect contributions of fireworks under significantly different emission patterns.

Therefore, the purpose of this work is to individually quantify the total, direct and indirect contributions of fireworks to size-resolved PM. A sampling campaign of PM_{10} and $PM_{2.5}$ was performed before, during, and after the CNY (as shown in Table S1) in a megacity in China. The physicochemical characteristics of the PM during this folk-custom festival were investigated, and the influence of fireworks on the physicochemical changes was also studied. The tracer species of fireworks were discussed and then used for the source identification. The total, direct and indirect

contributions of fireworks to PM were modelled using the Positive Matrix Factorization (PMF), Peak Analysis (PA) and Chemical Mass Balance (CMB) models. The quantitative assessment of the fireworks' direct and indirect impacts on the ambient PM gives an original contribution to understand the physicochemical characteristics and mechanisms during firework displays. The findings will aid in studies on similar high-intensity anthropogenic activities.

2 Methodology

2.1 Sampling

The PM_{10} and $PM_{2.5}$ samples were collected in Tianjin (a megacity in China). Tianjin, the largest harbour of Northern China, is a fast-growing and economically developed city that has a population of more than 12 million and has more than 1.5 million automobiles. The air quality of Tianjin has declined with rapid urbanisation and industrialisation. The sampling site is sited on the rooftop of a six-story building that is located in a mixed residential and commercial area in Tianjin. Usually, substantial degradation would occur during the firework displays in such a mixed area. The map of the sampling site was indicated in Fig. S1.

The sampling campaign of PM_{10} and $PM_{2.5}$ was performed from 30 January 2013 to 24 February 2013, including periods before, during, and after the CNY (until the Lantern Festival). The sampling periods and the corresponding Chinese lunar calendar were listed in Table S1. During the sampling periods, firework displays occurred for the celebration of the CNY holiday. For the period from CNY's Eve to the Lantern

Festival, fireworks are allowed in China, and numerous fireworks were consumed; thus, this period is defined as a heavy-firework period. For the period before CNY's Eve, sporadic fireworks might be set off, so it is defined as a light-firework period.

Based on our previous works and other related studies (Shi et al., 2009; Xue et al., 2010; Harrison et al., 2012; Tian et al., 2013a; Zhao et al., 2013 a, b), the $PM_{2.5}$ and PM_{10} (24 hour samples) were simultaneously collected on quartz-fibre filters and polypropylene-fibre filters using medium-volume air samplers (TH-150) at a flow rate of 100 L/min. The detailed information for the sampling and quality assurance/quality control (QA/QC) are available in the Supplementary Materials.

2.2 Chemical Analysis

The elemental compositions (Al, Si, Ca, V, Cr, Mn, Fe, Co, Cu, Zn, As and Pb) of the samples collected on the polypropylene-fibre filters were determined by inductively coupled plasma-mass spectrometry (ICP-AES) (IRIS Intrepid II, Thermo Electron). Ion chromatography (DX-120, DIONEX) was used to analyse the water-soluble ions (NO_3^-, SO_4^{2-}, Na^+, K^+ and Mg^{2+}) collected on the quartz-fibre filters. The organic carbon (OC) and elemental carbon (EC) concentrations of the samples on the quartz-fibre filters were determined by DRI/OGC carbon analysis, a technique based on the IMPROVE thermal/optical reflectance (TOR) protocol.

The background contamination was routinely monitored by blank tests. Enough blank tests were conducted and used to valid and correct the corresponding data. Certified reference materials (CRM, produced by National Research Center for

Certified Reference Materials, China) were used for quality assurance and quality control. Blanks and duplicate sample analyses were performed for nearly 10% of the samples. The pretreatment procedure, chemical analysis and QA/QC are described in detail in the Supplementary Materials and refer to our previous works and other related studies (Bi et al., 2007; Shi et al., 2009; Wu et al., 2009; Kong et al., 2010; Xue et al., 2010; Zhao et al., 2013 a, b).

In addition, scanning electron microscopy (SEM) determinations were performed by a JEOL JSM-7500F equipped with an X-ray energy dispersive spectrometer (EDS) to perform a morphological characterisation and chemical analysis of the individual particles.

2.3 Modelling approaches

2.3.1 Receptor models

Two widely used receptor models, Positive Matrix Factorisation (PMF) and Chemical Mass Balance (CMB), were applied to quantify the total (sum of the direct and indirect contributions), direct and indirect contributions of fireworks.

PMF is a useful factorisation methodology that can identify potential source categories and source contributions when the source profiles are not known. It identifies the source profile matrix F and quantifies the source contribution matrix G based on observations at the receptor site (X). Following Paatro and Tapper (1994), the PMF model can be represented in matrix form as:

$$\boldsymbol{X} = \boldsymbol{GF} + \boldsymbol{E}, \quad (1)$$

The elements of the source contribution matrix G and source profile matrix F are constrained to non-negative values for PMF. PMF uses the residual matrix elements (e_{ik}) and uncertainty estimates (σ_{ij}) to calculate a minimum Q value by using a weighed least square method, which is defined as:

$$Q(E) = \sum_{i=1}^{m} \sum_{j-1}^{n} (e_{ij} / \sigma_{ij})^2, \quad (2)$$

where σ_{ij} is the uncertainty of the j^{th} species in the i^{th} sample, which is used to weight the observations that include sampling errors, detection limits, missing data, and outliers (Paatero,2007). The goal of PMF is to minimise this function.

PM data from the different sizes ($PM_{2.5}$ and PM_{10}) were combined and inputted into PMF, as has been done in related works (Amato et al., 2009; Aldabe et al., 2011). The combined data showed satisfactory results, and further analysis demonstrated that the profiles of $PM_{2.5}$ and PM_{10} were similar in this work. Additionally, different numbers of factors and different Fpeak values were considered and tested when running PMF. The calculations were allowed to repeat ten times from ten pseudorandom starting points for each computation, to test if a global minimum point was reached. The error model code (EM=-14) and the uncertainties required for PMF were chosen according to the user's guide (Paatero, 2007).

Then, the CMB model was applied to quantify the individual contributions from the direct and indirect impacts of fireworks. CMB is also a widely used receptor model, for cases in which the number and profiles of sources are available (Watson et al., 1984; Chen et al., 2012). Similar to PMF, the CMB can be described as:

$$x_{ij} = \sum_{p=1}^{p} g_{ip} f_{pj} + e_{ij}, \quad (3)$$

where x_{ij} is the j^{th} species concentration measured in the i^{th} sample; f_{pj} is the j^{th} species mass fraction in the p^{th} source; g_{ip} is the contribution of the p^{th} source to the i^{th} sample; and e_{ij} is the residual (Hopke,2003). In contrast to PMF, except for x_{ij}, f_{pj} should also be available for the CMB model. USEPA CMB8.2 (USEPA, 2004) was applied in this work. The main performance indices of CMB are the reduced chi square (χ^2), percent mass (PM) and R square (R^2). Understanding the information of sources is important for the CMB modelling. In this work, a field survey of sources was performed before applying the CMB model, to determine the source categories.

2.3.2 Peak Analysis

In the present study, Peak Analysis was used to quantify the species abundances of the fireworks based on the observations of the PM and chemical species. This method was successfully applied to determine the profiles of the vehicle emissions (Ke et al., 2013). The highest and lowest PM or species concentrations were used to represent the peak and background observations, respectively. The peak period had the strongest fireworks density, whereas the background values corresponded to the lowest fireworks density. Then, the species abundances were obtained by normalising their concentrations with the corresponding PM concentrations, as follows (Ke et al, 2013):

$$F_j = \frac{C_{p,j} - C_{b,j}}{C_{p,PM} - C_{b,PM}}, \quad (4)$$

where F_j is the abundance (g per g of PM) for the j^{th} species, $C_{p,j}$ and $C_{b,j}$ are the j^{th} species concentrations ($\mu g/m^3$) in the peak observation and the background

observation, respectively; and $C_{p,PM}$ and $C_{b,PM}$ are the PM concentrations (μg/m^3) in the peak and the background observations, respectively.

The uncertainty (σ_{F_j}) of the j^{th} species abundance (F_j) was defined as follows (Ke et al, 2013):

$$\sigma_{F_j} = F_j \sqrt{(\frac{\sigma_{p,j}}{c_{p,j}})^2 + (\frac{\sigma_{b,j}}{c_{b,j}})^2}, \quad (5)$$

where $\sigma_{p,j}$ and $\sigma_{b,j}$ are the measurement uncertainties (μg/m^3) of the j^{th} species in the peak observation and the background observation, respectively. The results of the Peak Analysis method were employed to describe the profiles of the total fireworks.

3 Results and discussion

3.1 Physicochemical characteristics of PM_{10} and $PM_{2.5}$

The PM samples were acquired on two filters for each sampling day, so consistency tests play an important role in the QA/QC process. The comparisons between the concentrations measured on the polypropylene-fibre filters and those on the quartz-fibre filters were shown in Fig. S2. A satisfactory consistency (slopes close to unity and high correlations) were observed, indicating good quality assurance. Because the quartz-fibre filters tend to absorb water and be shredded during sampling handling (Cheng et al., 2011), concentrations on the polypropylene-fibre filters were used in the following discussion.

The concentrations of the PM_{10} and $PM_{2.5}$ in Tianjin during the sampling periods are summarised in Fig. S3. The average concentration of PM_{10} was 212.95 μg/m^3, and that of $PM_{2.5}$ was 140.59 μg/m^3, with an average ratio of $PM_{2.5}/PM_{10}$ of 0.66. The

$PM_{2.5}/PM_{10}$ values were 0.65 and 0.66 during the light-firework and heavy-firework periods, respectively. The T-test was used to analyse the difference between the $PM_{2.5}/PM_{10}$ values in the two periods, and the results indicated an insignificant difference with $p>0.05$. The PM_{10} and $PM_{2.5}$ concentrations were 148.74 $\mu g/m^3$ and 96.80 $\mu g/m^3$, respectively, during the light-firework period and 249.08 $\mu g/m^3$ and 165.23 $\mu g/m^3$, respectively, during the heavy-firework period. The highest concentrations were observed on CNY's Eve, when massive firework displays usually occur all over the country (Feng et al., 2012), indicating the huge influence of fireworks on the PM concentrations. Additionally, the concentrations of PM_{10} and $PM_{2,5}$ during non-firework period were 133.30 $\mu g/m^3$ and 83.98 $\mu g/m^3$, which were sampled from Tianjin in March and April, 2013. Compared with non-firework period, the PM levels during light-firework period were slightly higher and those during heavy-firework period were much higher.

The study of the chemical composition is critical for understanding the physicochemical characteristics of pollution during the folk-custom festival. The average concentrations of the chemical species in PM_{10} and $PM_{2.5}$ during the light-firework period and the heavy-firework period were exhibited in Fig. 1, and the abundance of the species (fractions of the species in PM) in PM_{10} and $PM_{2.5}$ were summarised in Fig. S4. According to Fig. 1 and Fig. S4, the crustal elements (Al, Si, Fe, and Ca), carbonaceous species (OC and EC) and several water-soluble ions (Cl^-, NO_3^- and SO_4^{2-}) were important species in PM_{10} and $PM_{2.5}$ during the sampling periods. The concentrations of OC were 9.84 and 15.58 $\mu g/m^3$ in PM_{10} and were 7.61

and 11.32 μg/m^3 in $PM_{2.5}$ during the light- and heavy-firework periods, respectively. The concentrations of EC were 5.59 (in PM_{10} during the light-firework period), 6.79 (in PM_{10} during the heavy-firework period), 4.20 (in $PM_{2.5}$ during the light-firework period) and 4.55 (in $PM_{2.5}$ during the heavy-firework period) μg/m^3. The ratio of OC/EC was higher during the heavy-firework period for both PM_{10} and $PM_{2.5}$, with values of 1.76 (light-firework) and 2.32 (heavy-firework) for PM_{10} and 1.81 (light-firework) and 2.49 (heavy-firework) for $PM_{2.5}$. Additionally, it was interesting to find that K^+ played an important role during the heavy-firework period, in contrast to its effect during the light-firework period. Compared with prior studies (Kong et al., 2010; Tian et al., 2013b), several differences can be observed in chemical compositions.

(Fig. 1)

In addition, for further characterisation, images and micrographs of the quartz-fibre filters were exhibited. Fig. S5 shows photos of the quartz filters with the PM_{10} and $PM_{2.5}$ samples for two cases: a normal day in the light-firework period and CNY's Eve in the heavy-firework period. A difference can be observed between the filters. Furthermore, Fig. S6 shows micrographs of $PM_{2.5}$ for the same days. There were many more particles for the samples from CNY's Eve than for those from the normal day, demonstrating the much higher concentration levels on CNY's Eve.

3.2 Influence of fireworks on the physicochemical characteristics of PM pollution

Comparing the mass concentrations and abundances of species during the

heavy-firework period with those during the light-firework period could help researchers learn more about the influence of this intensive human activity. As shown in Fig. 1, concentrations of most species (such as crustal elements, heavy metal species, carbonaceous species, Cl^-, Na^+, K^+, and Mg^{2+}) exhibited increasing trends during the heavy-firework period. It is believed that Al, Ca, Cr, Cu, Pb, Cl^-, Na^+, K^+, and Mg^{2+} might represent firework-related species. Potassium is one of the major components of fireworks because potassium compounds in black powder (commonly in the form perchlorate or chlorate) act as the main oxidisers during burning, with the corresponding chemical equations being $2KClO_3=2KCl+3O_2$ and $KClO_4=KCl+2O_2$. Ca compounds (such as calcium chloride and sulphate) and Cu compounds (such as copper chloride and oxide) give rise to orange and blue colourations, respectively. A Cr compound ($CuCr_2O_4$) is used as a catalyst for propellants. Cu, K, and Cr are used to provide silvery and glitter effects as well. Mg is a useful metallic fuel and is also used to produce sparks and crackling stars (in the form of the 50:50 Mg:Al alloy magnalium). Al also can be used alone as a common constituent for fuel, sparks and glitter effects. Pb can help to achieve steady and reproducible burning rates. Many components are in the form of perchlorate or chlorate, leading to high concentrations of Cl^-. The abruptly high emissions of these elements due to firework combustion can explain the high concentrations of these firework-related species in atmospheric PM during the heavy-firework period. It is noteworthy that certain firework-related heavy metals (Cr, Pb, Cu, etc.) are dangerous elements because of their toxicity and are forbidden by law in many countries. Such high concentrations in a short time,

312 especially in a place where a considerable number of people are gathered, might be of
313 concern.

314 Except for the directly firework-related species, an increase was also observed for
315 most of the crustal elements (such as Al, Si and Ca). Although Al and Ca might derive
316 from industrial and direct firework sources, the abrupt increase of crustal elements
317 might also be due to the resuspension of materials already deposited on the ground,
318 caused by pyrotechnic device explosions. Additionally, higher concentrations of K^+
319 and OC, which are good markers of biomass combustion, might imply the
320 contribution of biomass combustion during the heavy-firework period. The higher
321 concentrations of these indirect markers during the heavy-firework period can be
322 ascribed partly to the indirect influence of fireworks. The important contributions of
323 the resuspended dust and biomass combustion must be taken into consideration as
324 sources of PM in these firework events. Moreover, the mass ratios of NO_3^- to SO_4^{2-}
325 (NO_3^-/SO_4^{2-}) during the heavy-firework period were lower than the ratios during the
326 light-firework period. Similarly, lower NO_3^-/SO_4^{2-} during CNY was observed in
327 Beijing (Feng et al., 2012). The change in NO_3^-/SO_4^{2-} might be partly due to differing
328 formation mechanisms. Wang et al. (2007) reported the dominance of metal-catalysed
329 heterogeneous formation of sulphate during the firework period. Goodman et al.
330 (2001) reported a different formation mechanism for nitrate. However, the formation
331 of secondary particles might be influenced by considerable factors (such as
332 meteorological conditions and precursors) and is very complex.

333 Some of the species mentioned here require further study. SEM micrographs and

EDS spectra of particles on the normal day and on CNY's Eve were exhibited in Fig. S7. The individual-particle analysis showed a higher K level on CNY's Eve than on the normal day. Furthermore, K^+, Cr, and Mg^{2+} particularly stand out as species that have far higher concentrations during the heavy-firework period than that during the light-firework period. The H/L values (the ratios of the concentrations in the heavy-firework period to those in the light-firework period) of the K^+, Cr, and Mg^{2+} concentrations were 6.29, 5.52, 3.97 for PM_{10} and 5.78, 4.63, 6.32 for $PM_{2.5}$ (as shown in Fig. 1), respectively. The mass concentrations may not completely reflect the composition of PM, so a comparison of the species abundances was also performed. As shown in Fig. S4, the abundances of K^+, Cr, and Mg^{2+} were obviously higher during the heavy-firework period, with H/L values of 3.08, 4.44, 1.78 for PM_{10} and 2.68, 2.06 and 2.37 for $PM_{2.5}$, respectively. The high H/L values of the abundances can demonstrate the intensive influence of the fireworks on these species. For further investigation, the daily variations in the concentrations and abundances of the most firework-influenced species (K^+, Mg^{2+} and Cr) were shown in Fig. S8. Similar temporal patterns were observed for these species. Both the mass concentrations and abundances of K^+, Mg^{2+} and Cr showed sharp peaks for CNY's Eve for $PM_{2.5}$ and PM_{10}. Obvious increases also occurred on the fifth day of the Chinese lunar calendar and the Lantern Festival, which are important folk-custom days for fireworks. Thus, K^+, Mg^{2+} and Cr could indicate the influence of fireworks, which is important for further identification of the source categories of fireworks.

Species in PM may result from anthropogenic and natural sources. To focus the

356 characteristics of anthropogenic emissions, the non-sea-salt (nss) ions were calculated.
357 Assuming that all of the Na^+ ions were from sea salt, the concentrations of nss-SO_4^{2-},
358 nss-Cl^-, nss-K^+ and nss-Mg^{2+} in PM_{10} and $PM_{2.5}$ were calculated based on the
359 composition of average seawater. The relative mass concentrations of SO_4^{2-}, Cl^-, K^+
360 and Mg^{2+} to Na^+ are 0.252, 1.8, 0.037 and 0.119, respectively (Feng et al., 2012).
361 Nearly all SO_4^{2-} and K^+ (>98%) and most Mg^{2+} (>75%) ion in both PM_{10} and $PM_{2.5}$
362 are from non-sea-salt. It is interesting to find a higher percentage of nss-Cl^- in $PM_{2.5}$
363 (72%) than in PM_{10} (57%), indicating the stronger influence of anthropogenic
364 emissions on the Cl^- in fine PM. This result is reasonable because sea salt contributes
365 a higher fraction to the coarse fraction of PM (Keuken et al., 2013). To investigate the
366 anthropogenic impacts of fireworks, a comparison was conducted between nss-ions
367 during the light-firework and heavy-firework periods. The nss-SO_4^{2-} accounts for
368 more than 98% of the SO_4^{2-} in both the $PM_{2.5}$ and PM_{10}, and there was no obvious
369 difference ($p > 0.05$) during the two periods. The concentrations of nss-Cl^-, nss-K^+
370 and nss-Mg^{2+} as well as their percentages in the total ions were exhibited in Fig. S9.
371 For these three ions, much higher concentrations and higher percentages occurred
372 during the heavy-firework period, especially on CNY's Eve, with more than 88% of
373 the ions resulting from anthropogenic impacts. These results suggest the large
374 anthropogenic influence on Cl^-, K^+, Mg^{2+}, which may be mainly caused by fireworks
375 during the Chinese folk-custom festival; as a result, they were effective to indicate the
376 presence of fireworks. In the present work, the sources to Cl^- are complex, including
377 not only anthropogenic but also natural sources (Vassura et al., 2014). Additionally,

considering insufficient concentrations of Cr in the PM mass, K^+ and Mg^{2+} may be more powerful as tracers of fireworks for the following source apportionment, as indicated by related reports (Wang et al., 2007; Cheng et al., 2013).

3.3 Sources of PM

To quantitatively evaluate the total, direct and indirect impacts of fireworks on ambient PM, source apportionment of size-resolved PM samples was modelled by the PMF, Peak Analysis and CMB models in this section.

3.3.1 Total contributions of fireworks by PMF modelling

PMF was first applied to identify the possible source categories and to quantify their contributions to PM during the sampling periods. The variation in the Q values, actual condition based on the field survey, the estimated source profiles and source contributions, the correlations between measured and estimated concentrations were taken into consideration when judging the performance of PMF solutions. Finally, the five-factor solution and Fpeak=0.1 were determined for fitting. The fitting plot between the measured and estimated PM concentrations was exhibited in Fig. S10. The slope of the regression was 0.96, and the Pearson correlation coefficient was 0.98, suggesting perfect performance of PMF in this run (the estimated PM concentrations for most samples were similar to the measured concentrations).

The source profiles obtained by PMF are listed in Fig. 2 and Table S2. According to Fig. 2, Factor 1 exhibited high loadings for Al, Si, Ca (0.31, 0.35 and 0.63 in normalized source profiles as shown in Table S2), etc., which are associated with

crustal dust (Pant and Harrison et al., 2012). In Factor 2, relatively higher loadings of Al, Si and carbonaceous species were observed. Previous studies demonstrated that simultaneously high Al, Si and carbonaceous species might indicate coal combustion as the source category (Zhang et al., 2011; Pant and Harrison et al., 2012). Factor 3 correlates strongly with SO_4^{2-} and NO_3^-, consistent with source categories related to secondary particles (secondary sulphate and secondary nitrate) (Gao et al., 2011; Tian et al., 2013a). Factor 4 is mainly characterised by OC and EC (0.48 and 0.50 in normalized source profiles), which were indicative of vehicular exhaust (Pant and Harrison et al., 2012). The percentage contributions of these source categories were summarised in Fig. 2 as well.

(Fig. 2)

In Factor 5, K^+ presented obviously high weightings. As discussed above, K^+ may be a tracer of fireworks. And the higher loading of Mg^{2+} (0.65 in normalized source profiles in Table S2) and Cr (0.71 in normalized source profiles) in this factor might also indicate the impacts of fireworks. Furthermore, it is interesting to find the relatively higher weightings of other species, such as OC, Al, Si and Ca. Strong links with K^+ and OC could demonstrate biomass combustion (Cheng et al., 2013). Factor 5 was also associated with Al, Si and Ca, which are crustal elements. Biomass combustion might be indirectly caused by fireworks, which can occur when the fireworks are displayed and incinerated after display. Crustal elements might result from the resuspension of materials already deposited on the ground (caused by pyrotechnic device explosions). Therefore, Factor 5 represented the total influence of

422 fireworks, which might include the direct-firework contribution and indirect impacts
423 (biomass combustion and resuspended dust). PMF extracts source profiles and
424 quantifies contributions based on the temporal variation of the chemical species, so
425 source categories in one emission pattern might be identified as one factor. In this
426 work, direct fireworks, resuspended dust and biomass combustion caused by
427 fireworks may have similar emission patterns.

428 As exhibited in Fig. 2, the total influence of fireworks, including the direct-firework
429 and indirect impacts, contributed 19.29% to PM_{10} and 24.09% to $PM_{2.5}$ during the
430 entire sampling periods. The averaged percentage source contributions to PM_{10} and
431 $PM_{2.5}$ during the light-firework and heavy-firework periods, respectively, are
432 calculated and shown in Fig. 3. A large difference can be observed. During the
433 light-firework period, the total influence of fireworks contributed 4.28% to PM_{10} and
434 7.18% to $PM_{2.5}$; while during the heavy-firework period, the total influence of the
435 fireworks increased to rather high fractions (23.40% for PM_{10} and 29.66% for $PM_{2.5}$).
436 The time series of the percentage contributions of the total firework impacts on PM_{10}
437 and $PM_{2.5}$ were exhibited in Fig. 4, which could represent the trend of the total
438 firework impacts (including direct fireworks, resuspended dust and biomass
439 combustion). The most significant peak of the total firework contributions was
440 presented on CNY's Eve, indicating the heavy impacts of the total fireworks on this
441 day, although the contributions may be overestimated due to the uncertainties in the
442 results by PMF. In most cities in China, fireworks are allowed from CNY's Eve to the
443 Lantern Festival (namely, the heavy-firework period in this work). Numerous

fireworks were displayed on the night of CNY's Eve, as it is the most important celebration of the year. Another peak of firework contributions was observed on the Lantern Festival. The Lantern Festival is also an important festival in China and is the last day that fireworks are allowed. The variation in the firework contributions was consistent with the Chinese folk celebrations, which demonstrate the good performance of PMF for modelling the total firework contributions in this work.

(Fig. 3)

(Fig. 4)

3.3.2 Species abundances of the total firework impacts

In addition to PMF, Peak Analysis was also employed to better understand the total firework impacts. As discussed above, the profiles and contributions of the total firework impacts were determined by PMF for PM_{10} and $PM_{2.5}$. Furthermore, Peak Analysis (Ke et al., 2013) was employed in this section to investigate the species abundances of the total fireworks in terms of the observations. The species abundances of the total firework impacts obtained by the two independent methods (PMF and Peak Analysis) were exhibited in Fig. 5. Considering the complexity mentioned previously, the secondary ions were not included in the comparison. Comparing the firework profiles, the abundances of most chemical species by Peak Analysis were similar to the corresponding values by PMF. As shown in Fig. 5, the abundance of K^+, which is the main marker of direct-fireworks as discussed above, were consistent in the three firework profiles, with values of 16.34% by PMF, 15.21% by Peak Analysis for PM_{10} and 17.33% by Peak Analysis for $PM_{2.5}$. The Al, Si and Ca

(resuspended dust elements) as well as OC (marker of biomass combustion along with K^+) levels were also in agreement. The abundances of Al were 5.87%, 6.72% and 7.02%; Si were 9.87%, 10.07% and 11.85%; and OC were 6.32%, 5.87% and 6.60%, estimated by PMF, by Peak Analysis for PM_{10} and by Peak Analysis for $PM_{2.5}$, respectively. For a further investigation of the similarity among these profiles, regression analyses and correlation coefficients (R) were computed and shown in Fig. 5. It is visible from Fig. 5 that all of the correlation coefficients were greater than 0.9, suggesting that the total firework profiles obtained by PMF and by Peak Analysis were concordant. In addition, the firework profiles of $PM_{2.5}$ were similar with those of PM_{10}, implying that it is reasonable to introduce the combined dataset of $PM_{2.5}$ and PM_{10} into PMF.

(Fig. 5)

3.3.3 Contributions of the direct and indirect firework impacts

As discussed above, the total influence of the fireworks might include indirect impacts (resuspended dust and biomass combustion) and direct-fireworks. Thus, it is necessary to deeply evaluate the individual impacts of fireworks. In this work, the total firework profiles calculated by Peak Analysis were applied as the receptors in the CMB model, and the source profiles of three contributors (resuspended dust, biomass combustion and direct-fireworks) were incorporated into the model, to individually determine the direct and indirect impacts of fireworks. In this work, the source profiles of the resuspended dust were from our prior works in Tianjin (Zhang et al., 2011); the biomass combustion profiles were from speciate 4.0 of the US EPA;

and the firework profiles were taken from a reported work (Tsai et al., 2012). The performance indices of CMB in this work were summarised in Table S3. The values of the performance indices met the requirement, indicating that the results of CMB might be reliable.

The individual contributions to the total firework impacts (based on Peak Analysis) were exhibited in Fig. 3 and Table S3. According to the estimations, the percentage contributions of resuspended dust, biomass combustion and direct-fireworks were 36.82±8.37%, 14.08±2.82% and 44.44±8.26%, respectively, for PM_{10}, accounting for the total firework contribution. For $PM_{2.5}$, the percentage contributions were estimated to be 34.89±4.19% from resuspended dust, 16.60±3.05% from biomass combustion, and 52.54±9.69% from direct-fireworks. The sum of resuspended dust, biomass burning and direct-fireworks was >100% for $PM_{2.5}$ and < 100% for PM_{10}, however, they were in the range of the 80-120%, which met the requirement of the CMB. The results demonstrated that fireworks can lead to a comprehensive influence on the ambient PM. In addition to the direct-firework influence, resuspended dust and biomass combustion indirectly caused by fireworks should also be considered.

4 Conclusions

To quantify the total, direct and indirect impacts of fireworks, size-resolved PM samples were collected in a megacity in China. The sampling campaign covered a Chinese folk-custom festival (CNY), which provides a unique opportunity to quantify the contributions of fireworks under significantly different emission patterns. The

strong influence of fireworks on the physicochemical characteristics of atmospheric PM_{10} and $PM_{2.5}$ was observed. The highest PM concentrations were observed on CNY's Eve, when massive firework displays usually take place all over the country. The concentrations of most species (such as crustal elements, heavy metal species, carbonaceous species, Cl^-, Na^+, K^+, and Mg^{2+}) exhibited increased trends during the heavy-firework period. Among these, K^+, Mg^{2+} and Cr showed the most obvious increase, and the results of non-sea-salt ions demonstrated the anthropogenic influence on these species. K^+, Mg^{2+} and Cr can be good tracers for fireworks, especially for K^+ and Mg^{2+}, which had higher concentrations. Subsequently, source apportionment was conducted using receptor models. The total influence of fireworks was quantified by PMF, contributing higher fractions during the heavy-firework period than those during the light-firework period. The profiles of the total fireworks obtained by PMF and Peak Analysis were consistent, with higher abundances of K^+, Al, Si, Ca and OC. Finally, the individual contributions of the direct and indirect impacts of fireworks were determined by the CMB model based on profiles from Peak Analysis. The present study demonstrated that fireworks might lead to a comprehensive influence on the ambient PM. Both the direct influence and indirect impacts (resuspended dust and biomass combustion) caused by fireworks should be considered. The present work can be helpful in understanding the physicochemical characteristics and mechanisms of such high-intensity anthropogenic activities.

Acknowledgments

This study is supported by the National Natural Science Foundation of China (21207070 and 41375132), Special Funds for Research on Public Welfares of the Ministry of Environmental Protection of China (201409003) and the Ph.D. Candidate Research Innovation Fund of Nankai University.

References

Aldabe, J., Elustondo, D., Santamaría, C., Lasheras, E., Pandolfi, M., Alastuey, A., Querol, X., and Santamaría, J.M.: Chemical characterisation and source apportionment of PM2.5 and PM10 at rural, urban and traffic sites in Navarra (North of Spain), Atmos. Res., 1, 191-205, 2011.

Amato, F., Pandolfi, M., Escrig, A., Querol, X., Alastuey, A., Pey, J., Perez, N., and Hopke, P. K.: Quantifying road dust resuspension in urban environment by multilinear engine: a comparison with PMF2, Atmos. Environ., 17, 2770-2780, 2009.

Bi, X.H., Feng, Y.C., Wu, J.H., Wang, Y.Q., and Zhu, T.: Source apportionment of PM10 in six cities of northern China, Atmos. Environ., 41, 903-912, 2007.

Chen, W.A., Watson, J.G., Chow, J.C., Green, M.C., Inouye, D., and Dick, K.: Wintertime particulate pollution episodes in an urban valley of the Western US: a case study, Atmos. Chem. Phys., 12, 10051-10064, 2012.

Cheng, Y., Engling, G., He, K.B., Duan, F.K., Ma, Y.L., Du, Z.Y., Liu, J.M ., Zheng, M., and Weber, R.J.: Biomass burning contribution to Beijing aerosol, Atmos. Chem. Phys., 13, 7765-7781, 2013.

554 Cheng, Y., Zou, S.C., Lee, S.C., Chow, J.C. , Ho, K.F., Watson, J.G. , Han, Y.M.,
555 Zhang, R.J., Zhang, F., Yau, P.S., Huang , Y., Bai, Y. , and Wu, W.J.: Characteristics
556 and source apportionment of PM1 emissions at a roadside station, J. Hazard. Mater.,
557 195, 82-91, 2011.
558 Crespo, J., Yubero, E., Nicolás, J.F., Lucarelli, F., Nava, S., Chiari, M., Calzolai, G.:
559 High-time resolution and size-segregated elemental composition in high-intensity
560 pyrotechnic exposures, J. Hazard. Mater., 241-242, 82-91, 2012.
561 Ding, X., Zheng, M., Yu, L.P., Zhang, X.L., Weber, R.J., Yan, B., Russell, A.G.,
562 Edgerton, E.S., and Wang, X.M.: Spatial and Seasonal Trends in Biogenic
563 Secondary Organic Aerosol Tracers and Water-Soluble Organic Carbon in the
564 Southeastern United States, Environ. Sci. Technol, 42, 5171-5176, 2008.
565 Feng, J.L., Sun, P., Hu, X.L., Zhao, W., Wu, M.H., and Fu, J.M.: The chemical
566 composition and sources of PM 2.5 during the 2009 Chinese New Year's holiday in
567 Shanghai, Atmos. Res., 118, 435-444, 2012.
568 Gao, X., Yang, L., Cheng, S., Gao, R., Zhou, Y., and Xue, L.: Semi-continuous
569 measurement of water-soluble ions in PM 2.5 in Jinan, China: temporal variations
570 and source apportionments, Atmos. Environ., 45, 6048-6056, 2011.
571 Goodman, A.L., Bernard, E.T., and Grassian, V.H.: Spectro-scopic study of nitric acid
572 and water adsorption on oxide particles: enhanced nitric acid uptake kinetics in the
573 presence of adsorbed water, J. Phys. Chem. A, 105 (26), 6443-6457, 2001.
574 Hopke, P. K.: Recent developments in receptor modeling, J. Chemom., 17, 255-265,
575 2003.

576 Huang, K., Zhuang, G., Lin, Y., Wang, Q., Fu, J.S., Zhang, R., Li, J., Deng, C., and Fu,
577 Q.: Impact of anthropogenic emission on air quality over a megacity – revealed
578 from an intensive atmospheric campaign during the Chinese Spring Festival, Atmos.
579 Chem. Phys., 12, 11631–11645, 2012.
580 Ke, H.H., Ondov, J.M., and Rogge, W.F.: Detailed emission profiles for on-road
581 vehicles derived from ambient measurements during a windless traffic episode in
582 Baltimore using a multi-model approach, Atmos. Environ., 81, 280-287, 2013.
583 Keuken, M.P., Moerman, M., Voogt, M., Blom, M., Weijers, E.P., Röckmann , T., and
584 Dusek, U.: Source contributions to PM2.5 and PM10 at an urban background and a
585 street location, Atmos. Environ.,71, 26-35 ,2013.
586 Kong, S.F., Han, B., Bai, Z.P., Chen, L. Shi, J.W., and Xu, J.W.: Receptor modeling of
587 PM2.5, PM10 and TSP in different seasons and long-range transport analysis at a
588 coastal site of Tianjin, China, Sci. Total Environ., 408, 4681–4694, 2010.
589 Lin, Z. J. , Tao, J. , Chai, F. H., Fan, S. J., Yue, J. H., Zhu, L. H. , Ho, K. F.,and Zhang,
590 R. J.: Impact of relative humidity and particles number size distributionon aerosol
591 light extinction in the urban area of Guangzhou, Atmos. Chem. Phys., 13,
592 1115-1128, 2013.
593 Paatero, P., Tapper, U.: Positive Matrix Factorization: a non-negative factor model
594 with optimal utilization of error estimates of data values, Environmetrics, 5,
595 111-126, 1994.
596 Paatero, P.: User's guide for positive matrix factorization programs PMF2 and PMF3,
597 part 1-2: tutorial. Helsinki, Finland: University of Helsinki, 2007.

598 Pant, P., and Harrison, R.M.: Critical review of receptor modelling for particulate
599 matter: A case study of India, Atmos. Environ., 49, 1-12, 2012.
600 Robichaud, A. and Ménard, R.: Multi-year objective analyses of warm season
601 ground-level ozone and PM 2.5 over North America using real-time observations
602 and Canadian operational air quality models, Atmos. Chem. Phys., 14, 1769–1800,
603 2014.
604 Sarkar, S., Khillare, P.S., Jyethi, D.S., Hasan, A., Parween, M.: Chemical speciation of
605 respirable suspended particulate matter during a major firework festival in India. J.
606 Hazard. Mater., 184, 321–330, 2010.
607 Shen, G.F., Tao, S., Wei, S.Y., Chen, Y.C., Zhang, Y.Y., Shen, H.Z., Huang, Y., Zhu, D.,
608 Yuan, C.Y., Wang, H.C., Wang, Y.F., Pei, L.J., Liao, Y. L., Duan, Y.H., Wang, B.,
609 Wang, R., Lv, Y., Li, W., Wang, X.L., and Zheng, X.Y.: Field Measurement of
610 Emission Factors of PM, EC, OC, Parent, Nitro-, and Oxy- Polycyclic Aromatic
611 Hydrocarbons for Residential Briquette, Coal Cake, and Wood in Rural Shanxi,
612 China, Environ. Sci. Technol, 47, 2998−3005, 2013.
613 Shi, G.L., Feng, Y.C., Zeng, F., Li, X., Zhang, Y.F., and Wang, Y.Q.: Use of a
614 Nonnegative Constrained Principal Component Regression Chemical Mass Balance
615 Model to Study the Contributions of Nearly Collinear Sources, Environ. Sci.
616 Technol, 43, 8867-73, 2009.
617 Shi, Y.L., Zhang, N., Gao, J.M., Li, X., Cai, Y.Q.: Effect of fireworks display on
618 perchlorate in air aerosols during the Spring Festival, Atmos. Environ., 45,
619 1323-1327, 2011.

620 Tian, Y.Z., Shi, G.L., Han, S.Q., Zhang, Y.F., Feng, Y.C., Liu, G.R., Gao, L.J., Wu, J,H.,
621 and Zhu, T.: Vertical characteristics of levels and potential sources of water-soluble
622 ions in PM10 in a Chinese megacity, Sci. Total Environ., 447, 1-9, 2013a.
623 Tian, Y.Z., Xiao, Z.M., Han, B., Shi, G.L., Wang, W., Hao, H.Z., Li, X., Feng, Y.C.,
624 and Zhu, T: Seasonal Study of Primary and Secondary Sources of Carbonaceous
625 Species in PM10 from Five Northern Chinese Cities, Aerosol Air Qual. Res., 13,
626 148–161, 2013b.
627 Tsai, H.H., Chien, L.H., Yuan, C.S., Lin, Y.C., Jen, Y.H., and Ie, I.R.: Influences of
628 fireworks on chemical characteristics of atmospheric fine and coarse particles
629 during Taiwan's Lantern Festival, Atmos. Environ., 62 , 256-264, 2012.
630 U.S. Environmental Protection Agency: EPA-CMB8.2 Users Manual, U.S. EPA,
631 office of Air Quality Planning and Standards, Research Triangle Park, NC 27711,
632 2004.
633 Vassura, I., Venturini, E., Marchetti, S., Piazzalunga, A., Bernardi, E., Fermo, P.,
634 Passarini, F.: Markers and influence of open biomass burning on atmospheric
635 particulate size and composition during a major bonfire event, Atmos. Environ., 82 ,
636 21-225, 2014.
637 Vecchi, R., Bernardoni, V., Cricchio, D., D'Alessandro, A., Fermo, P., Lucarelli, F.,
638 Nava, S., Piazzalunga, A., and Valli, G.: The impact of fireworks on airborne
639 particles, Atmos. Environ., 42, 1121-1132, 2008.
640 Wang, Y., Zhuang, G.S., Xu, C., and An, Z.S.: The air pollution caused by the burning
641 of fireworks during the lantern festival in Beijing, Atmos. Environ., 41 , 417-431,

642 2007.
643 Watson, J. G., Cooper, J. A., and Huntzicker, J. J.: The effective variance weighting
644 for least squares calculations applied to the mass balance receptor model, Atmos.
645 Environ., 18, 1347-1355, 1984.
646 Wu, L., Feng, Y.C., Wu, J.H., Zhu, T., Bi, X.H., Han, B., Yang, W.H., and Yang, Z.Q.:
647 Secondary organic carbon quantification and source apportionment of PM10 in
648 Kaifeng, China, J. Environ. Sci., 21, 1353-1362, 2009.
649 Xue, Y.H., Wu, J.H., Feng, Y.C., Dai, L., Bi, X.H., and Li, X.: Source Characterization
650 and Apportionment of PM10 in Panzhihua, China, Aerosol Air Qual. Res., 10,
651 367-77, 2010.
652 Zhang, Y.F., Xu, H., Tian, Y.Z., Shi, G.L., Zeng, F., Wu, J.H., Zhang, X.Y., Li, X., Zhu,
653 T., and Feng, Y.C.: The study on vertical variability of PM10 and the possible
654 sources on a 220 m tower, in Tianjin, China, Atmos. Environ., 45, 6133-6140, 2011.
655 Zhao, P. S., Dong, F., He, D., Zhao, X.J., Zhang, X.L., Zhang, W.Z., Yao, Q. and Liu,
656 H.Y.: Characteristics of concentrations and chemical compositions for PM2.5 in the
657 region of Beijing, Tianjin, and Hebei, China, Atmos. Chem. Phys., 13, 4631–4644,
658 2013a.
659 Zhao, X. J., Zhao, P. S., Xu,, Meng, W., Pu, W. W., Dong, F., He, D. , and Shi, Q. F.:
660 Analysis of a winter regional haze event and its formation mechanism in the North
661 China Plain, Atmos. Chem. Phys., 13, 5685-5696, 2013b.
662 Zheng, M., Salmon, L.G., Schauer, J.J., Zeng, L.M., Kiang, C.S., Zhang, Y.H., and
663 Cass, G.R.: Seasonal trends in PM2.5 source contributions in Beijing, China, Atmos.

664 Environ., 39, 3967-3976, 2005.

665

666

Figure captions

Fig. 1. The averaged concentrations of the chemical species in PM_{10} and $PM_{2.5}$ during the light-firework period and the heavy-firework period.

Fig. 2. Source profiles ($\mu g/m^3$) and percentage source contributions (%) estimated by PMF for PM_{10} and $PM_{2.5}$.

Fig. 3. The total influence of fireworks on PM_{10} and $PM_{2.5}$ (%) during the light-firework and heavy-firework periods, estimated by PMF (column chart), and the individual percentage contributions to the total firework impacts estimated by CMB based on Peak Analysis (pie chart).

Fig. 4. The daily percentage contributions of the total firework impacts to PM_{10} and $PM_{2.5}$, estimated by PMF.

Fig. 5. Profiles of fireworks (g/g) estimated by PMF for PM_{10} and $PM_{2.5}$, Peak Analysis for PM_{10} and Peak Analysis for $PM_{2.5}$, and the regression plots between these profiles.

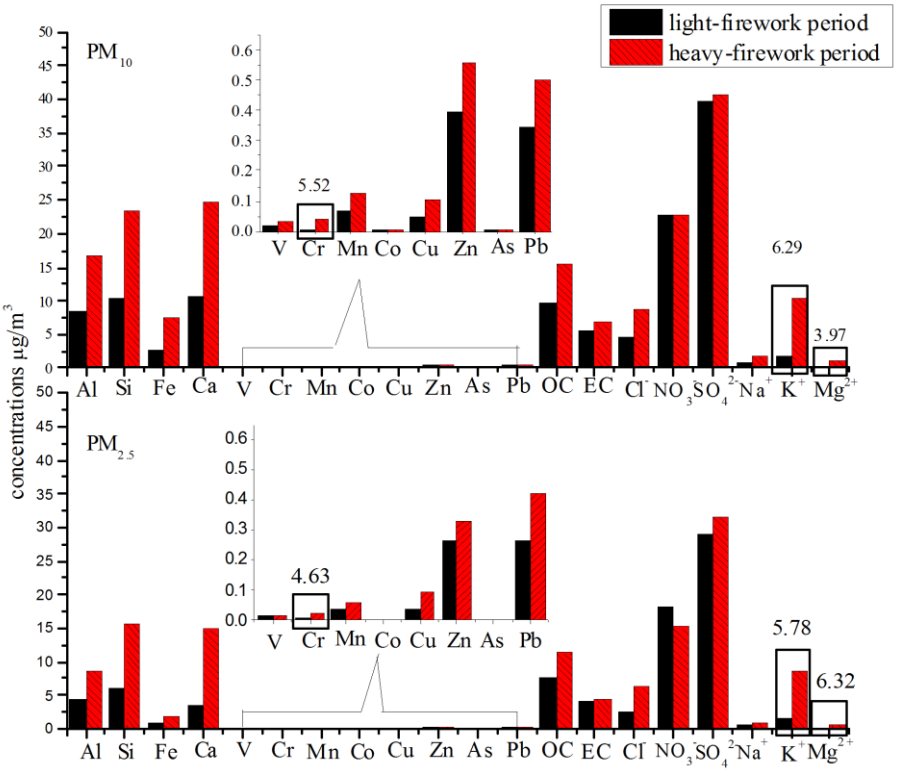

693

694 **Fig. 1**

695

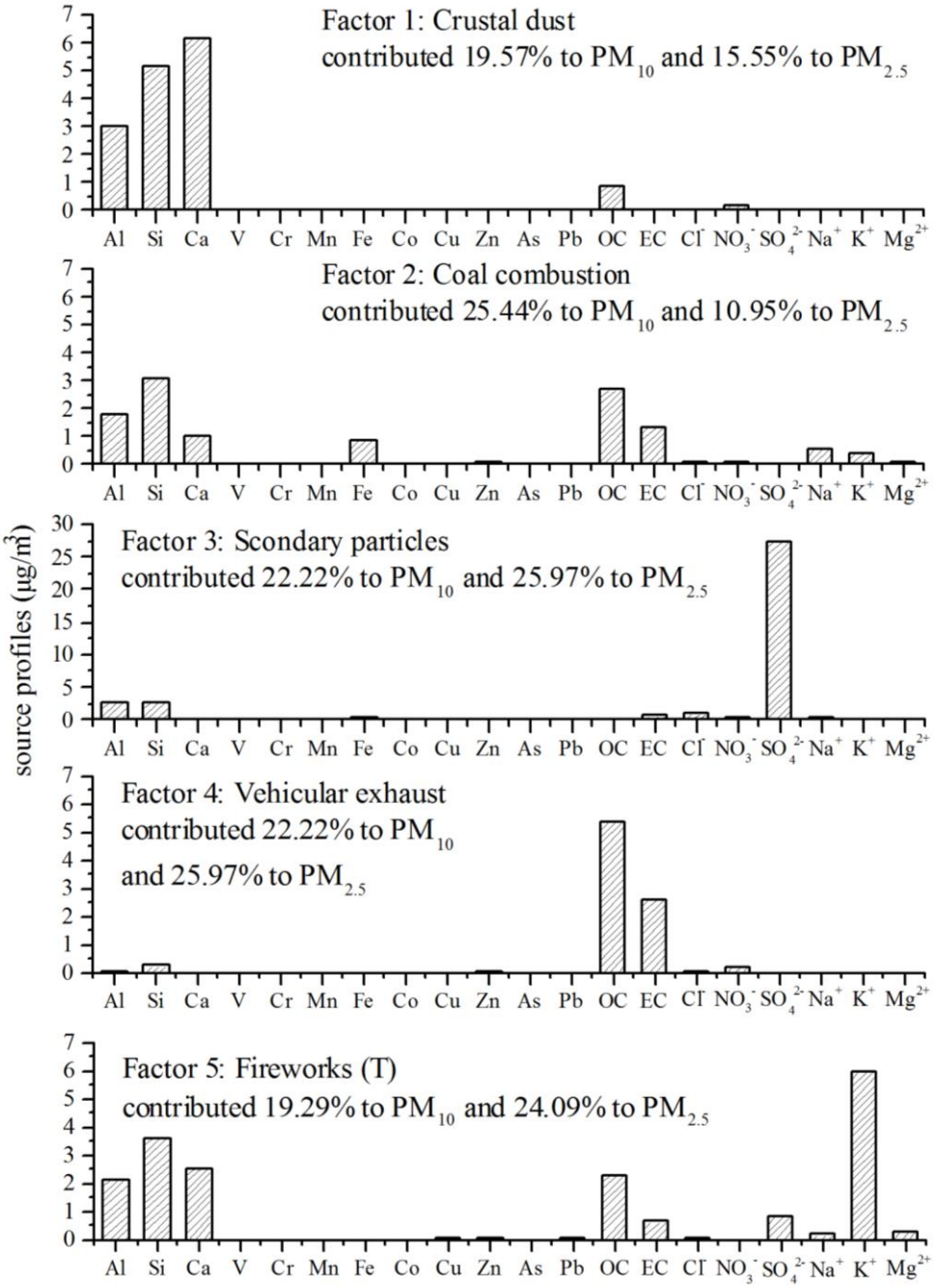
source profiles (μg/m3)
Factor 1: Crustal dust
contributed 19.57% to PM10 and 15.55% to PM2.5
Factor 2: Coal combustion
contributed 25.44% to PM10 and 10.95% to PM2.5
Factor 3: Scondary particles
contributed 22.22% to PM10 and 25.97% to PM2.5
Factor 4: Vehicular exhaust
contributed 22.22% to PM10
and 25.97% to PM2.5
Factor 5: Fireworks (T)
contributed 19.29% to PM10 and 24.09% to PM2.5
Al Si Ca V Cr Mn Fe Co Cu Zn As Pb OC EC Cl- NO3- SO42- Na+ K+ Mg2+

Fig. 2

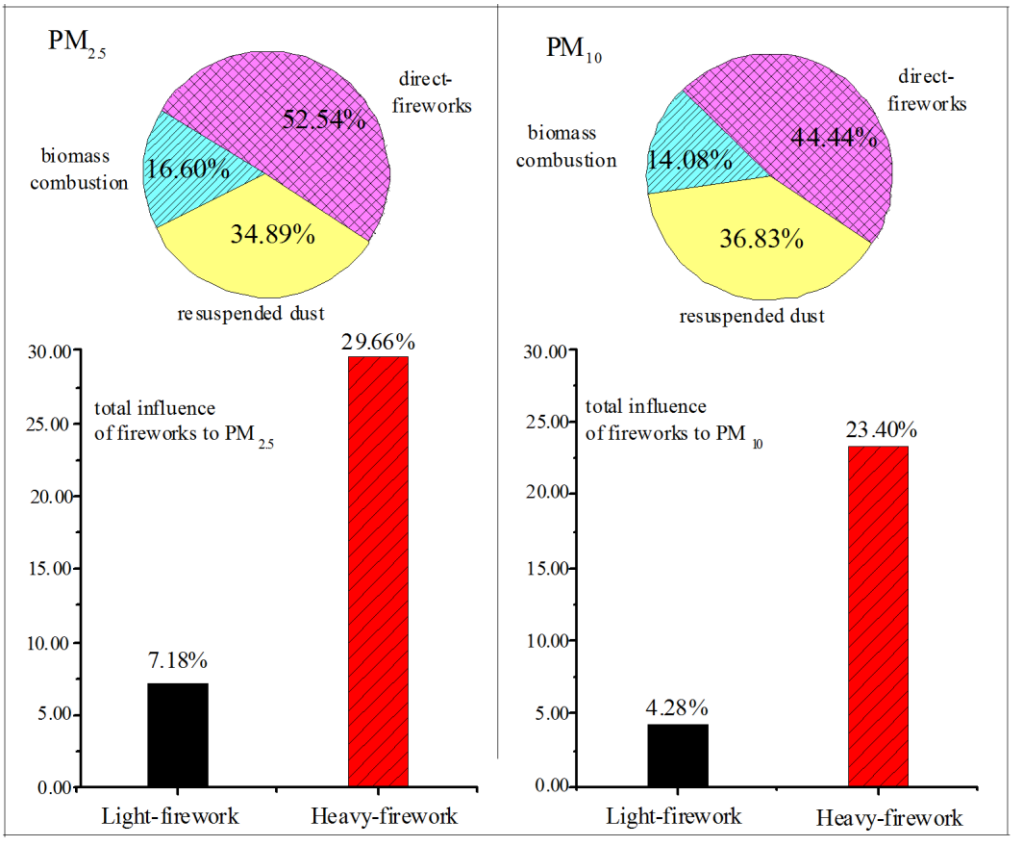

699

700 **Fig. 3**

701

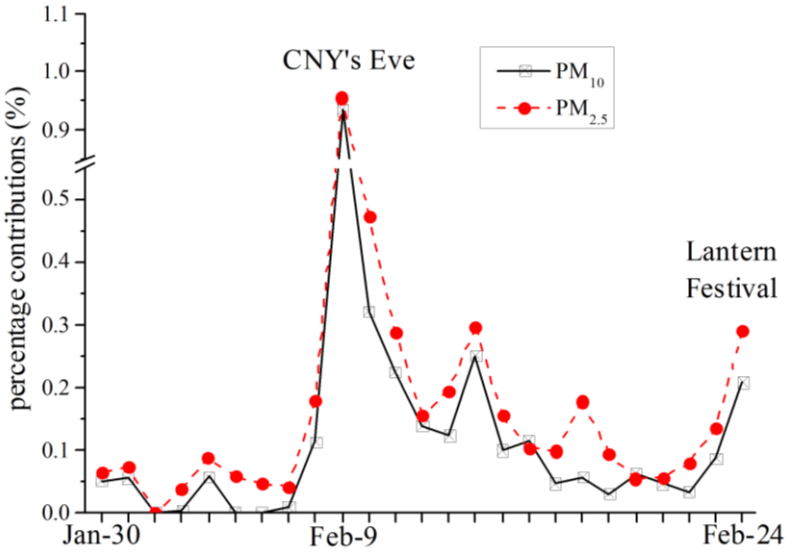
CNY's Eve
PM10
PM2.5
Lantern
Festival
percentage contributions (%)
1.1
1.0
0.9
0.5
0.4
0.3
0.2
0.1
0.0
Jan-30
Feb-9
Feb-24

Fig. 4

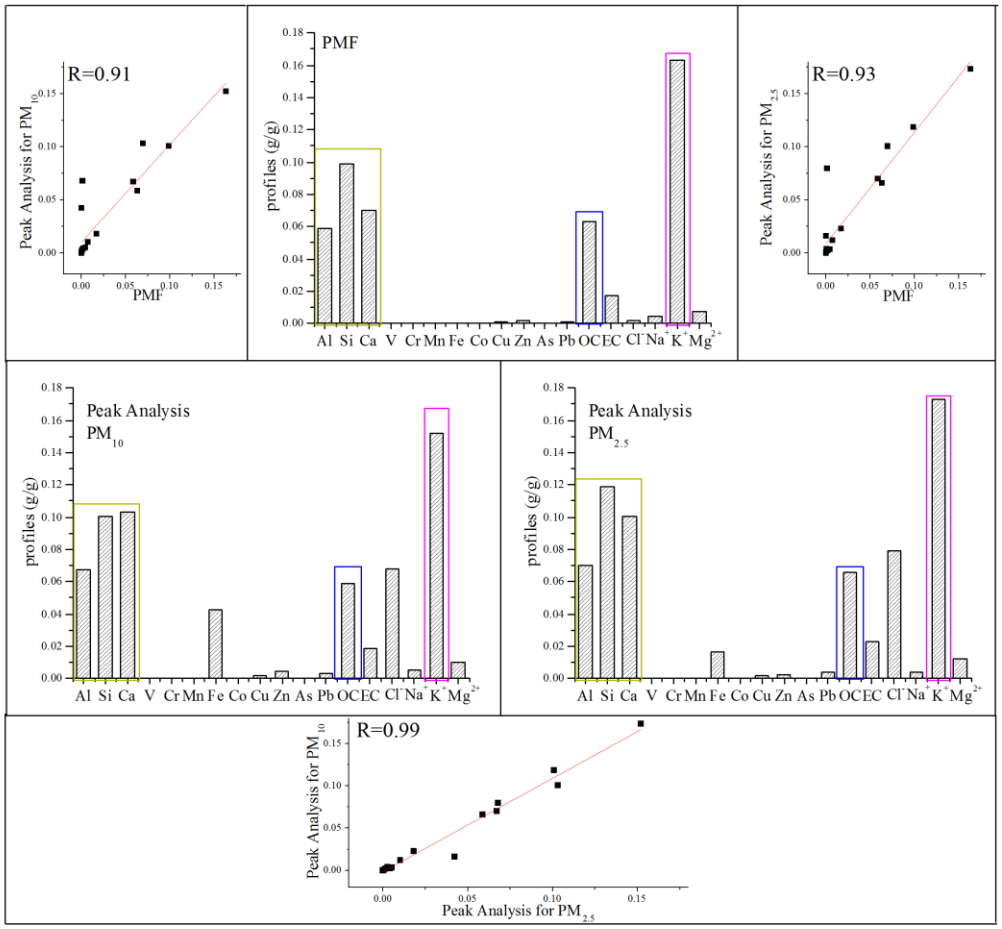
R=0.91
Peak Analysis for PM10
PMF
PMF
profiles (g/g)
Al Si Ca V Cr Mn Fe Co Cu Zn As Pb OC EC Cl- Na+ K+ Mg2+
R=0.93
Peak Analysis for PM2.5
PMF
Peak Analysis
PM10
profiles (g/g)
Al Si Ca V Cr Mn Fe Co Cu Zn As Pb OC EC Cl- Na+ K+ Mg2+
Peak Analysis
PM2.5
profiles (g/g)
Al Si Ca V Cr Mn Fe Co Cu Zn As Pb OC EC Cl- Na+ K+ Mg2+
R=0.99
Peak Analysis for PM10
Peak Analysis for PM2.5

705

706 **Fig. 5**